Anal. Bioanal. Electrochem., Vol. 14, No. 5, 2022, 510-522

Analytical & Bioanalytical Electrochemistry

2022 by CEE
www.abechem.com

Full Paper

A New Nanostructure Approach based on $Pr(OH)_3$/GQD and Imidazolium Ionic Liquid for Voltammetric Analysis of Tramadol

Afsaneh L. Sanati, and Farnoush Faridbod*

Center of Excellence in Electrochemistry, School of Chemistry, College of Science, University of Tehran, Tehran, Iran

*Corresponding Author, Tel.: +982161113813

E-Mail: faridbodf@ut.ac.ir

Received: 9 February 2022 / Received in revised form: 5 May 2022 / Accepted: 13 May 2022 / Published online: 31 May 2022

Abstract- Today, remarkable growth in the generation and abuse of drugs lead to the need for fast, simple, selective, and sensitive methods for their detection. Tramadol is one of the most abused drugs that can make addiction. A highly conductive and highly sensitive voltammetric method is developed for the determination of tramadol based on a 1-methyl-3-butyl imidazolium bromide/praseodymium hydroxide-graphene quantum dots nanocomposite modified carbon paste electrode (1-M-3-BBr/$Pr(OH)_3$-GQD/CPE). According to the obtained voltammograms, the 1-M-3-BBr/$Pr(OH)_3$-GQD/CPE exhibits high catalytic activity on the oxidation signal of tramadol. Tramadol shows an irreversible anodic oxidation peak in the potentials of ~1170 mV and ~1230 mV at the surface of a modified and unmodified CPE, respectively. Square wave voltammogram signals confirmed that the oxidation current of tramadol was increased linearly with its concentration in the range of 9.0×10^{-9}-3.0×10^{-4} mol L^{-1} with a detection limit of 3.0×10^{-9} mol L^{-1}. Finally, the 1-M-3-BBr/$Pr(OH)_3$-GQD/CPE was effectively used for the determination of tramadol in some real samples with an acceptable selectivity.

Keywords- Tramadol; Praseodymium hydroxide-graphene quantum dots; 1-methyl-3-butyl imidazolium bromide; Voltammetry; Electrochemical sensor

1. INTRODUCTION

The remarkable growth in the generation and abuse of drugs lead to the need for fast, simple, selective, and sensitive detection methods. Tramadol is one of the most abused drugs

that can make addiction. Initially, tramadol was used as an analgesic for mild to moderate pain but its abuse led to addiction [1]. Extreme use of tramadol may cause side effects such as increased heart rate, shortness of breath, seizures, and weakness [2]. To date, several analytical techniques have been developed for the detection of tramadol, such as gas chromatography (GC) [3], UV-Vis and fluorescence spectroscopy [4,5], high-performance liquid chromatography (HPLC) [6,7], mass spectrometer detection [8,9], solid-phase extraction [10,11], thin layer chromatography [12,13], and many other methods. Nonetheless, many of these analytical methods are needed to be time-consuming and are limited by the requirement of expensive tools, expert users, and preservation. Therefore, the need for an easy, fast, accurate, and reliable method for measuring tramadol in real samples is still felt. Electrochemical methods are one of the most reliable methods due to their relative simplicity, high efficiency, and low cost for the determination of tramadol. So far, many studies have been done to analyze tramadol electrochemically [14-17].

Over the past decade, with the advent and expansion of nanotechnology, many improvements in drugs and pharmaceutical electroanalysis have been seen [18-27]. Also, recent developments in the field of synthesis nanomaterials and nanocomposites suggested many technological advances for the detection of addiction drugs. Due to the attendance of unique properties in nano-size materials, the sensors that are designed based on nanotechnology, can behave with great sensitivity, lessen detection time, and low limits of detection. Materials with dimensions of less than 1 to 100 nm include a large surface area and quantum confinement size effects, as well as increased surface reactivity, electrical conductivity, and magnetic properties. Another feature of nanomaterials is their properties which can be modified by changing their size, and shape, making a composition of the surface with suitable functionalization. According to this, it is possible to improve the electronic, magnetic, spectroscopic, light-scattering, and conductive properties of nanomaterials by engineering the structural parameters. Furthermore, the application of nanoparticles as modifiers of sensors in combination with other materials has led to improved sensitivity and selectivity detection of drugs and pharmacological components [26-28]. So far, many of nanomaterials were applied as electrode modifiers for the detection of tramadol such as $NiFe_2O_4$/graphene nanocomposite [16], SiO_2@Fe_3O_4 [29], gold-carbon nanotube nanocomposite [30], gold nanoparticles [31], multi-wall carbon nanotube (MWCNT) [32], and conductive polymeric ionic liquid/Ni nanocomposite [33].

Graphene quantum dot (GQD) is a carbon-based nanomaterial and is composed with two strategies: bottom-up and top-down [34]. In the bottom-up routs, were used of a series of chemical reactions starting from small organic molecules to prepared GQD. Also, in top-down techniques, were used of the decomposition of suitable carbonaceous precursors for prepared GQD [39]. GQDs have some exclusively strange chemical/ physical properties, such as high conductivity, large surface area, low toxicity, biocompatibility [36] solubility, functionality,

two-dimensionality, among many others compounds [27]. In addition, the electronic/ photonic/chemical properties of GQDs can be improved effectively by chemical doping, which is widely used in the carbon nanomaterials field and this results in new phenomena and unanticipated functions [37].

On the other side, it should be noted that today due to the unique properties and significant chemical reactivity of rare earth oxide nanoparticles, they are used as modifiers also, because they have more electron layers and thus lead to better electron transfer. Therefore, in this paper praseodymium oxide as one of the lanthanides was used.

Light rare earth elements including La, Ce, Pr, and Nd have generally similar properties. Beside cerium compounds, praseodymium-based materials have also attracted great attention as luminescent materials, catalysts, high-k gate dielectric materials, and optical filters. Previously studies showed that $Pr(OH)_3$ nanostructures have high affinity and selective adsorption of the organic compound with amine ($-NH_2$) functional groups [38]. High selectivity can be attributed to the large effective surface area of the nanostructure, plentiful hydroxyl groups, and basic sites on the $Pr(OH)_3$ surface.

To the best of our knowledge, has not been reported an electrochemical sensor for the detection of tramadol based on $Pr(OH)_3$–GQD nanocomposite as an electrode modifier.

The purpose of the present study was the synthesis of GQD through a simple method and then preparing $Pr(OH)_3$-GQD nanocomposite and using it as a modifier in carbon paste electrode for electrochemical determination of tramadol.

2. EXPERIMENTAL

2.1. Materials and Reagents

All chemicals and reagents with analytical grades and high purities including praseodymium nitrate ($Pr(NO_3)_2.6H_2O$), sodium carbonate (Na_2CO_3), and glucose were purchased from Merck chemical company. Tramadol, graphite powder, sodium hydroxide, paraffin, and phosphoric acid were purchased from Sigma-Aldrich.

2.2. Synthesis of Pr_2O_3 nanoparticle

Pr_2O_3 nanoparticles were prepared by optimized precipitation and decomposition route which was reported by Pourmortazavi [37]. For this purpose, praseodymium nitrate and sodium carbonate were used as initial reagents. In this work, an aqueous solution (0.1 mol L^{-1}) of praseodymium nitrate ($Pr(NO_3)_2.6H_2O$) and a solution (0.1 mol L^{-1}) of sodium carbonate (Na_2CO_3) were prepared. The Na_2CO_3 solution was then slowly added into $Pr(NO_3)_2.6H_2O$ solution at room temperature with 0.2 ml/min feeding flow rate. Then, a light green precipitate is formed. The light green product was centrifuged at 5800 rpm for 8 min and washed three

times with distilled water and ethanol. The obtained product was calcined at 650 °C in air atmosphere for 4 h. Finally, the dark brown powder resulted.

2.3. Synthesis of $Pr(OH)_3$-GQD nanocomposite

$Pr(OH)_3$-GQD nanocomposites were synthesized via the hydrothermal method. Briefly, 1 g of glucose was mixed with 0.1 g of pre-synthesized Pr_2O_3 nanoparticles and then was dissolved in 20 mL of deionized water. The product solution was then transferred to a Teflon-lined autoclave and heated at 180 °C for 10 h to yield $Pr(OH)_3$-GQD nanocomposites. After cooling to room temperature, the final product was collected by centrifugation and the powders were dispersed in 10 mL of water for further studies.

2.4. Preparation of 1-M-3-BBr/$Pr(OH)_3$-GQD/CPE

1-M-3-BBr/$Pr(OH)_3$-GQD/CPE was prepared by mixing of 0.05 g $Pr(OH)_3$-GQD and 0.9 g graphite powder in the presence of a suitable amount of paraffin oil and 11-M-3-BBr as binders. The obtained paste is input into the end of the glass tube in the presence of a copper wire as a conductive matter.

2.5. Real samples

Injection samples from a local pharmaceutical factory and serum samples from a healthy person were used for the investigation of 1-M-3-BBr/$Pr(OH)_3$-GQD/CPE ability for tramadol electroanalysis in a real matrix. Plasma sample was obtained from the Iranian Blood Transfusion Center. A certain amount of the plasma sample was treated by adding several microliters of nitric acid (0.1 M) to precipitate its protein content and stirring for 1 min. Then, the sample was centrifuged at 3000 rpm for 15 min. The supernatant was separated, diluted, and used for the analysis. The injection sample was used without any pretreatment except dilutions with distilled or buffer solutions.

3. RESULTS AND DISCUSSION

3.1. Characterization of praseodymium hydroxide-graphene quantum dots

Figure 1A shows TEM images of $Pr(OH)_3$-GQD nanocomposite with spherical core-shell shape with core of $Pr(OH)_3$ and shell of GQD and Figure 1B shows TEM images of GQD nano-sheets. Also, the EDX analysis of $Pr(OH)_3$-GQD showed Pr, O and C elements that is agree with $Pr(OH)_3$-GQD nanocomposite (Figure 1C).

For more investigation, we recorded the XRD pattern of $Pr(OH)_3$-GQD and obtained signals is presented in Figure 2. The presence XRD is matched with reference pattern of $Pr(OH)_3$ with Code No. 01-083-2304.

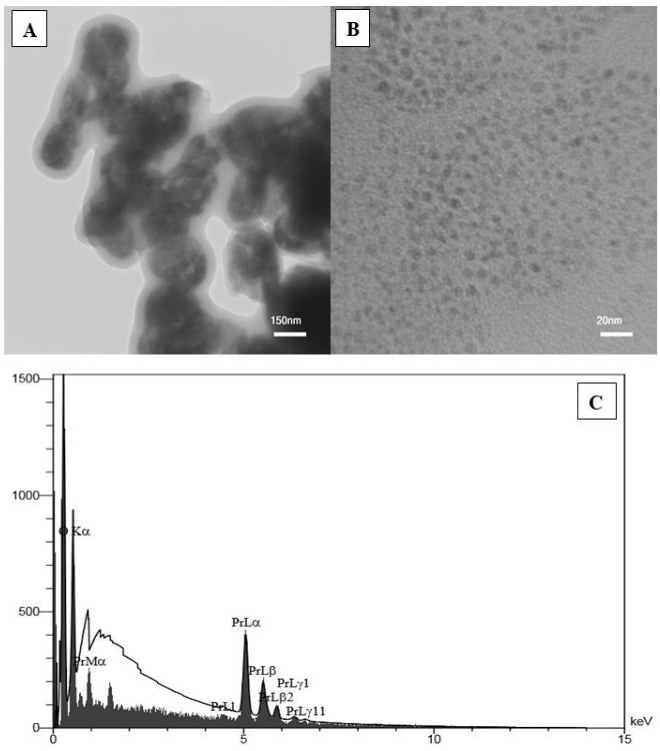

Figure 1. A) TEM image of $Pr(OH)_3$-GQD nano-hybrid; B) TEM image of GQD nano-sheets; C) EDX analysis of $Pr(OH)_3$-GQD nano-hybrid

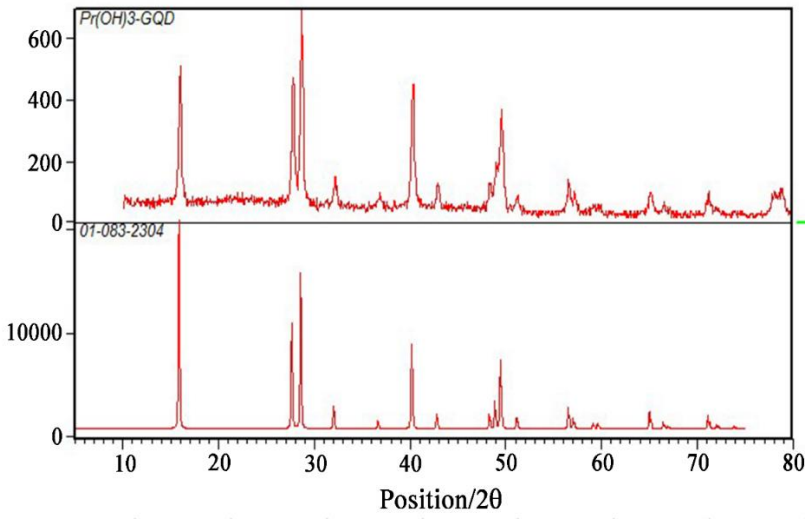

Figure 2. XRD pattern of $Pr(OH)_3$-GQD nano-hybrid

3.2. Electro-oxidation of tramadol at a surface 1-M-3-BBr/Pr(OH)-GQD/CPE

According to the previous published papers [40] and Scheme 1 mechanism, it found that electro-oxidation process of tramadol is related to the pH value and this factor optimized in the first step.

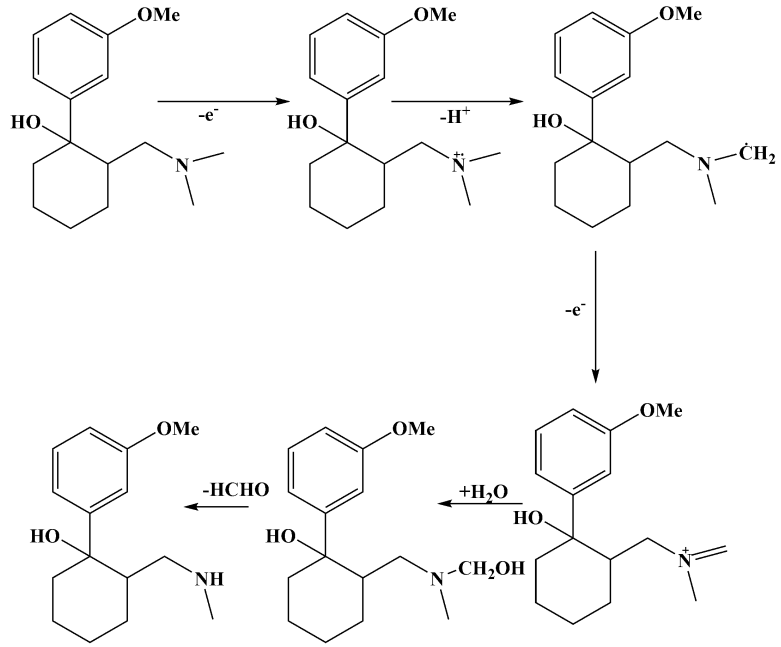

Scheme 1. Electro-oxidation mechanism of tramadol [39]

Figure 3 shows that the oxidation potential of tramadol shifted negatively with increasing the pH. A slope of -67.4 mV between oxidation potential of tramadol and pH is obtained that is agrees with equal value of proton and electron for an electroactive system. On the other hand, the peak current increased after moving of pH=7.0 to pH=8.0 and reduces after this pH (Figure 3 insert). Therefore, the pH=8.0 was used as best experimental condition and the supporting electrolyte in all voltammetric determination of tramadol.

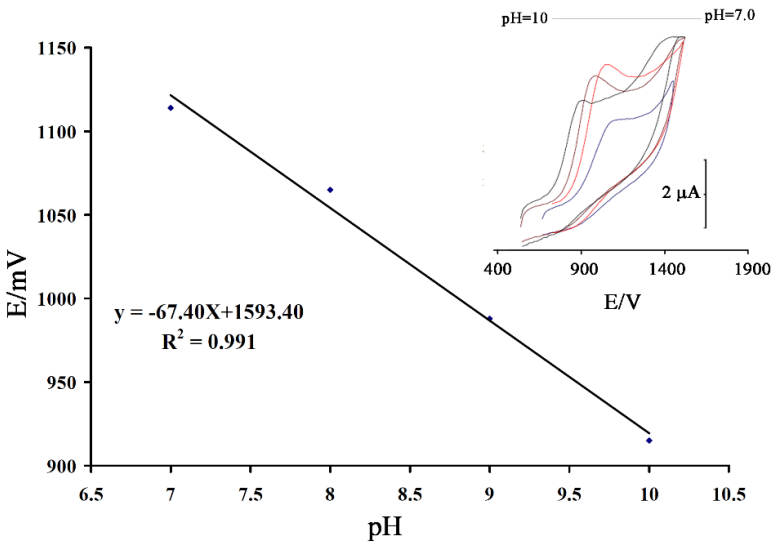

Figure 3. The E_p *vs.* pH curve for electro-oxidation of 450 µmol L^{-1} taramdol; insert: cyclic voltammograms of 450 µM taramdol at a surface of 1-M-3-BBr/$Pr(OH)_3$-GQD/CPE

The cyclic voltammograms of 400.0 µM tramadol was recorded on the 1-M-3-BBr/Pr(OH)$_3$-GQD/CPE (curve a), 1-M-3-BBr/CPE (curve b), Pr(OH)$_3$-GQD/CPE (curve c) and carbon paste electrode (curve d) for investigation of electrocatalytic properties of the 1-M-3-BBr and Pr(OH)$_3$-GQD nanocomposite at the surface of carbon paste electrode (Figure 4). At the unmodified electrode, the response of tramadol oxidation is weak and only an irreversible wave (peak potential ~1230 mV and peak current 0.87 µA is observed (curve d). At the Pr(OH)$_3$-GQD/CPE, the current of tramadol oxidation increased (2.12 µA) and the peak potential reduced (1190 mV) simultaneously. On the other hand, the oxidation signal of tramadol at a surface of 1-M-3-BBr/CPE showed an irreversible signal with oxidation current of 2.51 µA and oxidation potential of 1185 mV) that is better than of previous modified (curve c) and unmodified electrode (curve d). Finally, the oxidation signal of tramadol at a surface of 1-M-3-BBr/Pr(OH)$_3$-GQD/CPE appeared at a potential ~1170 mV and oxidation current 3.34 µA that shifted to the less positive than of other electrodes with better sensitivity. This improving in quality of 1-M-3-BBr/Pr(OH)$_3$-GQD/CPE can be relative to high conductivity and large specific surface area of 1-M-3-BBr and Pr(OH)$_3$-GQD that confirmed with current density investigation data (Figure 4 insert).

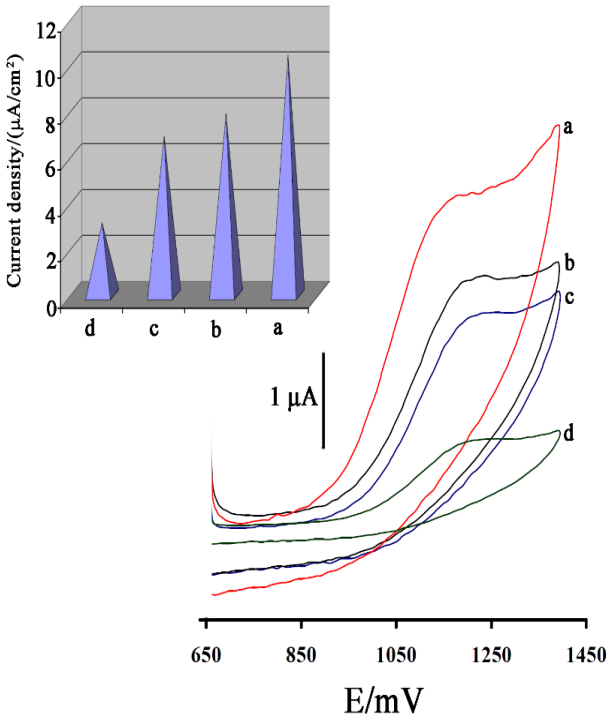

Figure 4. Cyclic voltammograms of 400 µM tramadol at four different electrodes: 1-M-3-BBr/Pr(OH)$_3$-GQD/CPE (a), 1-M-3-BBr/CPE (b), Pr(OH)$_3$-GQD/CPE (c) and CPE (d) Voltammetric conditions: scan rate of 100 mV s^{-1} in pH 8.0 phosphate buffer (0.1 mol L^{-1})

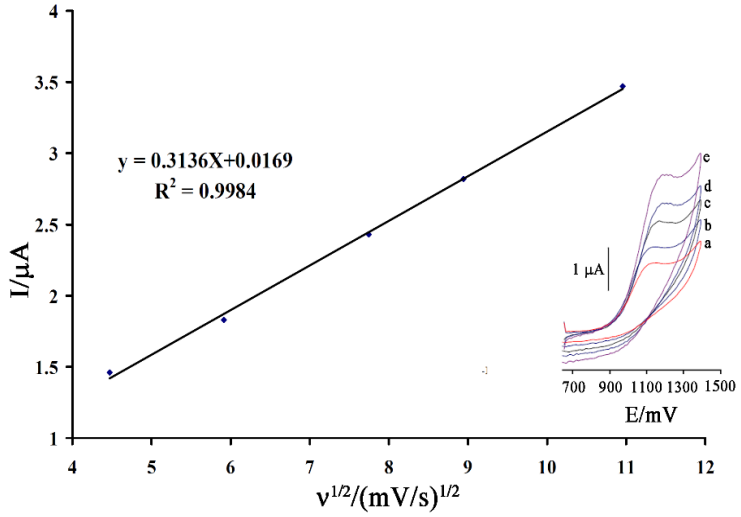

Figure 5. The plot of electrooxidation of tramadol with $\nu^{1/2}$; Cyclic voltammograms of tramadol (400.0 µmol L^{-1}) obtained in 0.1 M phosphate buffer (pH 8.0) employing varying scan rates (mV s^{-1}): (1–11) 20, 35, 60, 80 and 120

In the next step and for investigation the nature of tramadol electro-oxidation at a surface of the 1-M-3-BBr/Pr(OH)$_3$-GQD/CPE, the cyclic voltammograms of 400 µM tramadol are recorded at scan rates range between 20-120 mV s^{-1} (Figure 5 insert). The oxidation currents of tramadol are proportional to the $\nu^{1/2}$ (Figure 5) that indicate the reaction of tramadol oxidation is controlled by diffusion of tramadol on the surface of the 1-M-3-BBr/Pr(OH)$_3$-GQD/CPE.

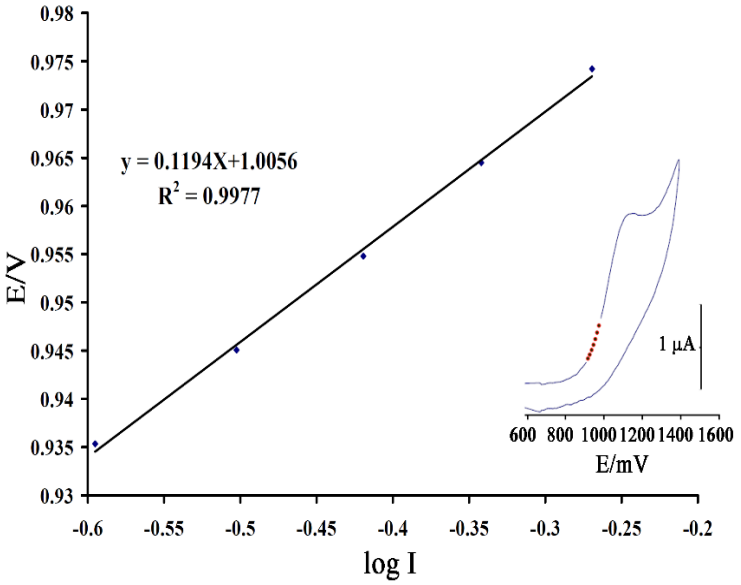

Figure 6. Tafel Plot for electro-oxidation of 400 µmol L^{-1} tramadol at a surface of 1-M-3-BBr/Pr(OH)$_3$-GQD/CPE with scan rate 35 mV/s

The Tafel investigation was used for obtain information about the rate-determining step (Figure 6). The Tafel plot was recorded in Figure 6 in the Tafel region of the cyclic voltammogram and using slope of this plot and Tafel equation [2.3RT/(1-α)nF], we calculated the value of α equal to 0.52.

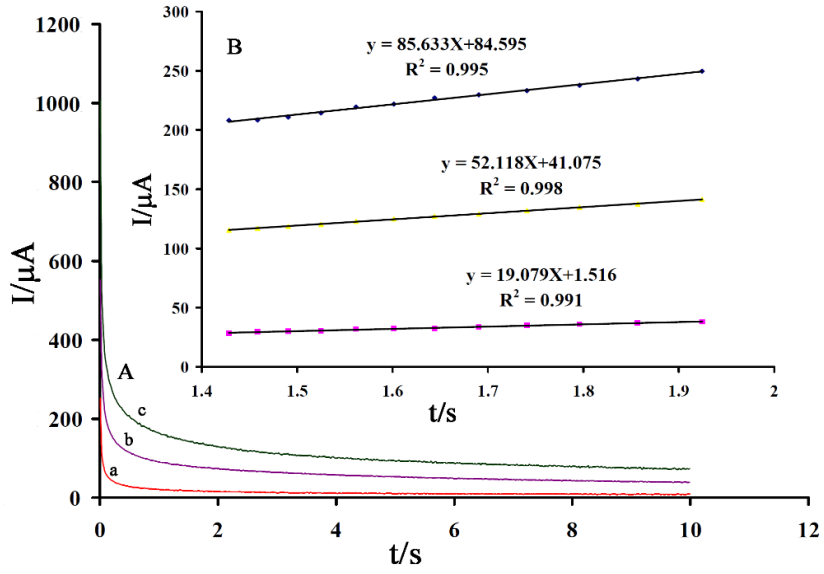

Figure 7. A) Chronoamperograms obtained at 1-M-3-BBr/Pr(OH)$_3$-GQD/CPE in the presence of a) 500; b) 700 and c) 900 µmol L^{-1} tramadol at pH 8.0. B Cottrell's plot for the data from the chronoamperograms

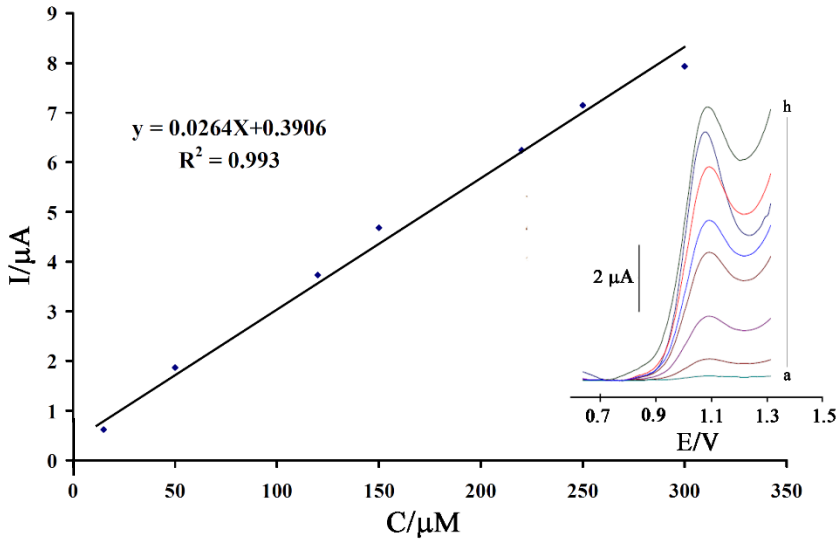

Figure 8. Plots of the peak current as a function of tramadol concentration; insert: square wave voltammograms of 1-M-3-BBr/Pr(OH)$_3$-GQD/CPE in pH 8.0 containing different concentrations of taramadol (from a-h) solutions of: 0.009; 15.0; 50.0, 120.0; 150.0; 220.0; 250.0 and 300.0 µmol L^{-1} tramadol, respectively

The oxidation behavior of tramadol was studied on a surface of 1-M-3-BBr/Pr(OH)$_3$-GQD/CPE by the chronoamperometric method (Figure 7A). The diffusion coefficient factor of tramadol was determined by the slopes of Cottrell plots and Cottrell equation as shown in Figure 7B. Using slopes of figure 7B, the diffusion coefficient of tramadol was determined to be 3.1×10^{-5} cm^2 s^{-1}.

The effect of tramadol concentration on the oxidation current of drug at a surface of 1-M-3-BBr/Pr(OH)$_3$-GQD/CPE was examined by changing the concentration of tramadol from 9.0×10^{-9}- 3.00×10^{-4} mol L^{-1} (Figure 8) with detection limit of 3.0×10^{-9} mol L^{-1} (LOD = $3S_b/m$) by square wave voltammetry method (frequency 12 Hz).

The stability of 1-M-3-BBr/Pr(OH)$_3$-GQD/CPE for analysis is crucial and must be check before real sample analysis. The stability of the 1-M-3-BBr/Pr(OH)$_3$-GQD/CPE was checked by keeping sensor buffer solution pH 9.0 for ten days and then the square wave voltammograms was recorded for 25 μmol L^{-1} tramadol and compared with square wave voltammograms obtained in the same solution before immersion. The results showed low changing in current and potential that confirmed good stability of sensor.

The selectivity of 1-M-3-BBr/Pr(OH)$_3$-GQD/CPE was investigated for analysis of 30 μmol L^{-1} tramadol as a new sensor with an acceptable relative error <5% for determination of tramadol. The results showed that the 750-fold for glucose, fructose, alanine, Li^+, K^+, F^-, Na^+ and phenyl alanine and 700-fold for citric acid and ascorbic acid did not affect the selectivity. The presence data suggesting highly selectivity of 1-M-3-BBr/Pr(OH)$_3$-GQD/CPE as an novel voltammetric sensor toward the determination of tramadol.

The square wave voltammetric method was used for analysis of tramadol in injection and pharmaceutical serum samples using the standard addition strategy. The obtained data toward analysis of tramadol in real samples are present in Table 1 and confirmed the good ability of 1-M-3-BBr/Pr(OH)$_3$-GQD/CPE for determination of tramadol in real samples.

Table 1. Determination of tramadol in drug samples (n=3)

Sample	Added tramadol (μmol L^{-1})	Expected tramadol (μmol L^{-1})	Found tramadol (μmol L^{-1})	Recovery for tramadol (%)
Injection	---	---	2.11±0.18	---
	10.00	12.11	12.08±0.22	99.75
Pharmaceutical serum	---	---	<limit of detection	---
	5.00	5.00	5.18±0.23	103.6

4. CONCLUSION

$Pr(OH)_3$ nanostructures shows high efficient and selective adsorption of the organic compound with amine ($-NH_2$) functional groups such as tramadol. Due to the good electrical conductivity and large surface area of $Pr(OH)_3$-GQD nanocomposite and 1-M-3-BBr (room temperature ionic liquid), the 1-M-3-BBr/$Pr(OH)_3$-GQD/CPE was fabricated as new electrochemical sensor for the sensitive determination of tramadol. It is a novel platform by coupling a nanostructure lanthanide nanocomposite and ionic liquid for modification of electrode toward analysis of tramadol. The 1-M-3-BBr/$Pr(OH)_3$-GQD/CPE showed a linear dynamic range between 9.0×10^{-9}-3.0×10^{-4} mol L^{-1} with a detection limit of 3.0×10^{-9} mol L^{-1} for analysis of tramadol and successfully used for the analysis of the drug in real samples.

Acknowledgments

The authors gratefully acknowledge the Research Council of University of Tehran for financial support of this work.

Conflicts of interest

The authors declare that they have no competing interests.

REFERENCES

[1] D. H. Epstein, K. L. Preston, and D. R. Jasinski, Biological Psychology 73 (2006) 90.
[2] M. S. Kazemi, J. Anal. Chem. 70 (2015) 1330.
[3] M. Abbasian, M. Balali-Mood, S.A. Mozaffari, and H. S. Amoli, J. Separation Sci. 39 (2016) 4449.
[4] Q. H. Zhao, C. P. Chen, T. T. Pang, L. M. Du, Y. A. N. Li, J. H. Xie, and Y. L. Fu, J. Chilean Chem. Soc. 60 (2015) 2659.
[5] B. De Backer, F. Renardy, R. Denooz, and C. Charlier, J. Anal. Toxicol. 34 (2010) 599.
[6] M. A. Hilal, and K. M. Mohamed, J. Chromat. Sci. 52 (2014) 1186.
[7] Z. Esmaeili, S. Mohammadi, A. Nezami, M. R. Rouini, Y. H. Ardakani, H. Lavasani, and M. Ghazi-Khansari, Biomedicine & Pharmacotherapy 91 (2017) 251.
[8] G. A. McMillin, S. J. Marin, K. L. Johnson-Davis, B. G. Lawlor, and F. G. Strathmann, American J. Clin. Pathology 143 (2015) 234.
[9] J. Wang, Z. Yang, and J. Lechago, Biomed. Chromat. 27 (2013) 1463.
[10] T. Madrakian, A. Afkhami, H. Mahmood-Kashani, and M. Ahmadi, Talanta 105 (2013) 255.
[11] F. Bevalot, C. Bottinelli, N. Cartiser, L. Fanton, and J. Guitton, J. Anal. Toxicol. 38 (2014) 256.
[12] K. Ferenczi-Fodor, Z. Végh, and B. Renger, TrAC Trends in Anal. Chem. 25 (2006) 778.

[13] W. D. S. Solomon, P. R. V. Anand, R. Shukla, R. Sivakumar, and R. Venkatnarayanan, Int. J. Chem. Tech. Res. 2 (2010) 1188.
[14] T. Madrakian, S. Alizadeh, M. Bahram, and A. Afkhami, Ionics 23 (2016) 1005.
[15] M. A. Mohamed, S. A. Atty, N. N. Salama, C. E. Banks, Electroanalysis 29 (2017) 1038.
[16] A. Afkhami, H. Khoshsafar, H. Bagheri, and T. Madrakian, Anal. Chim. Acta 831 (2014) 50.
[17] A. Shafaat, and F. Faridbod, Anal. Bioanal. Electrochem. 14 (2022) 319.
[18] A. L. Sanati, H. Karimi-Maleh, A. Badiei, P. Biparva, and A. A. Ensafi, Mater. Sci. Eng. C 35 (2014) 379.
[19] V. Arabali, M. Ebrahimi, M. Abbasghorbani, V. K. Gupta, M. Farsi, M. R. Ganjali, and F. Karimi, J. Mol. Liq. 213 (2016) 312.
[20] K. Khoshnevisan, H. Maleki, E. Honarvarfard, H. Baharifar, M. Gholami, F. Faridbod, B. Larijani, R. Faridi Majidi, and M. R. Khorramizadeh, Microchim. Acta 186 (2019) 1.
[21] K. Khoshnevisan, H. Baharifar, F. Torabi, M. Sadeghi Afjeh, H. Maleki, E. Honarvarfard, H. Mohammadi, S. M. Sajjadi-Jazi, S. Mahmoudi-Kohan, F. Faridbod, B. Larijani, F. Saadat, R. Faridi Majidi, and M. R. Khorramizadeh, Anal. Bioanal. Chem. 413 (2021) 1615.
[22] M. Habibi-Kool-Gheshlaghi, F. Faridbod, M. K. Mosammam, and M. R. Ganjali, Curr. Anal. Chem. 15 (2019) 423.
[23] L. Anvari, S. M. Ghoreishi, F. Faridbod, and M. R. Ganjali, Anal. Lett. 54 (2021) 2509.
[24] K. Khoshnevisan, E. Honarvarfard, F. Torabi, H. Maleki, H. Baharifar, F. Faridbod, B. Larijani, and M. R. Khorramizadeh, Clin. Chim. Acta 501 (2020) 112.
[25] M. K. Mosammam, M. R. Ganjali, M. Habibi-Kool-Gheshlaghi, and F. Faridbod, Curr. Anal. Chem. 15 (2019) 443.
[26] A. L. Sanati, and F. Faridbod, Int. J. Electrochem. Sci. (2017) 7997.
[27] A. L. Sanati, F. Faridbod, and M. R. Ganjali, J. Mol. Liq. 241 (2017) 316.
[28] H. Karimi-Maleh, F. Karimi, Y. Orooji, G. Mansouri, A. Razmjou, A. Aygun, and F. Sen, Scientific Reports 10 (2020) 1.
[29] A. Afkhami, H. Ghaedi, T. Madrakian, M. Ahmadi, and H. Mahmood-Kashani, Biosens. Bioelectron. 44 (2013) 34.
[30] N. F. Atta, R. A. Ahmed, H. M. A. Amin, A. Galal, Electroanalysis 24 (2012) 2135.
[31] B. J. Sanghavi, and A. K. Srivastava, Anal. Chim. Acta 706 (2011) 246.
[32] A. Babaei, A. R. TaheriI, and M. Afrasiabi, J. Brazilian Chem. Soc. 22 (2011) 1549.
[33] E. Molaakbari, A. Mostafavi, H. Beitollahi, and Z. Tohidiyan, Talanta 171 (2017) 25.
[34] X. Tong, Q. Wei, X. Zhan, G. Zhang, and S. Sun, Catalysts 7 (2016) 1.
[35] S. Paulo, E. Palomares, and E. Martinez-Ferrero, Nanomaterials 6 (2016) 9.
[36] F. Chen, W. Gao, X. Qiu, H. Zhang, L. Liu, P. Liao, W. Fu, and Y. Luo, Frontiers in Laboratory Medicine 1 (2017) 192.

[37] S. M. Pourmortazavi, M. Rahimi-Nasrabadi, M. Aghazadeh, M. R. Ganjali, M. Sadeghpour Karimi, and P. Norouzi, J. Electron. Mater. 46 (2017) 4627.
[38] T. Zhai, S. Xie, X. Lu, L. Xiang, M. Yu, W. Li, C. Liang, C. Mo, F. Zeng, T. Luan, and Y. Tong, Langmuir 28 (2012) 11078.
[39] A. Ahmed Hathoot, M. Elsayed Fahmy, M. Abdel Azzem, Int. J. Chem. Mater. Sci. 1 (2013) 45.
[40] S. Chitravathi, and N. Munichandraiah, J. Electroanal. Chem. 764 (2016) 93.